

**Cooling of trapped ions by resonant charge exchange**Sourav Dutta<sup>\*,†</sup> and S. A. Rangwala*Raman Research Institute, C. V. Raman Avenue, Sadashivanagar, Bangalore 560080, India*

(Received 22 June 2017; published 6 April 2018)

The two most widely used ion cooling methods are laser cooling and sympathetic cooling by elastic collisions (ECs). Here, we demonstrate another method of cooling ions that is based on resonant charge exchange (RCE) between the trapped ion and the ultracold parent atom. Specifically, trapped  $\text{Cs}^+$  ions are cooled by collisions with cotrapped, ultracold Cs atoms and, separately, by collisions with cotrapped, ultracold Rb atoms. We observe that the cooling of  $\text{Cs}^+$  ions by Cs atoms is more efficient than the cooling of  $\text{Cs}^+$  ions by Rb atoms. This signals the presence of a cooling mechanism apart from the elastic ion-atom collision channel for the Cs-Cs<sup>+</sup> case, which is cooling by RCE. The efficiency of cooling by RCE is experimentally determined and the per-collision cooling is found to be two orders of magnitude higher than cooling by EC. The result provides the experimental basis for future studies on charge transport by electron hopping in atom-ion hybrid systems.

DOI: [10.1103/PhysRevA.97.041401](https://doi.org/10.1103/PhysRevA.97.041401)

**Introduction.** The cooling and trapping of dilute gases, both neutral and charged, have enabled extremely precise and controlled experimentation with these systems [1,2]. The simultaneous trapping and cooling of atoms and ions results in an ion-atom hybrid system that allows for exciting experimental possibilities. The hybrid system has lent itself to studies of low-energy ion-atom collisions [3–6], charge-exchange reactions [3,5,7,8], sympathetic cooling of ions [4,9–11], cold chemical reactions [12], three-body processes [13], nondestructive ion detection methods [14], vibrational state cooling of molecular ions [15], etc., and holds promise for studies on charge transport [16,17], ion mobility [18], mesoscopic molecular ions [19], ion-atom photoassociation [20], and Feshbach resonance [21].

In these ion-atom hybrid systems, the ions are either laser cooled or sympathetically cooled by collisions with ultracold atoms. Elastic collisions (ECs) are present in all ion-atom hybrid systems, and therefore understanding them has attracted attention [4–6,9–11]. Recent experiments have studied the dependence of ion cooling on the size of the atomic ensemble and the atom-ion mass ratio [9–11]. Theoretical models [9,11,22–26] have also been developed to describe the cooling of trapped ions by ECs with cold atoms. In addition, another mechanism for the cooling of ions by resonant charge exchange (RCE) has been proposed [9,17] but no experimental evidence of this cooling mechanism has yet been provided. In this Rapid Communication, we experimentally show the “swap cooling” of ions based on RCE between the trapped ion and the cotrapped, ultracold, parent atom. Such swap cooling is restricted to homonuclear systems, where it offers promising prospects. We determine the efficiency of cooling by RCE with respect to cooling by EC for trapped  $\text{Cs}^+$  ions in ultracold Cs atoms and find the former to be higher. Our result confirms

and quantifies experimentally the role of RCE in ion cooling by trapped parent atoms.

The demonstration of cooling by RCE is also the first step towards the experimental realization of theoretical proposals [16,17] on the study of charge transport in the ultracold Na-Na<sup>+</sup> system and on studies of ion mobility [18]. The benefit of experiments with optically dark ions, e.g., Na<sup>+</sup>, Rb<sup>+</sup>, Cs<sup>+</sup>, etc., is that complications in the ion-atom collision process due to the presence of ions in the excited state [7,12] can be avoided. However, dark ions cannot be laser cooled and therefore low-energy collision experiments with such systems are scarce, although collisions in the keV range have been studied extensively [27,28]. It is only recently that low-energy ( $\lesssim 1$  eV) collisions were studied in the Rb-Rb<sup>+</sup> system [9] and the Na-Na<sup>+</sup> system [10], and the sympathetic cooling of trapped dark ions by collisions with the parent neutral atoms was demonstrated. For such homonuclear systems, it was proposed by Ravi *et al.* [9] that the sympathetic ion cooling could be due to (i) ECs between the fast ion and ultracold atoms or (ii) RCE between a fast ion and an ultracold atom, in which case the postcollision ion is essentially at rest [see Fig. 1(a)], or a combination of both. The individual contribution of (i) and (ii) and therefore the role of RCE in the ion cooling process, essential for the physics proposed in Ref. [16], is yet to be shown experimentally.

To achieve this, we cool  $^{133}\text{Cs}^+$  ions trapped in a Paul trap by collisions with ultracold  $^{133}\text{Cs}$  atoms trapped in a magneto-optical trap (MOT) and, separately, by collisions with ultracold  $^{85}\text{Rb}$  atoms trapped in a MOT. We observe that the cooling of  $\text{Cs}^+$  ions by Cs atoms is more efficient than the cooling of  $\text{Cs}^+$  ions by Rb atoms. This cannot be explained by ion cooling models that consider only ECs between ions and atoms. The faster cooling in the Cs-Cs<sup>+</sup> case is attributed to RCE between Cs atoms and  $\text{Cs}^+$  ions. We experimentally determine the efficiency of cooling by RCE and find the per-collision cooling to be two orders of magnitude higher than cooling by EC. This is remarkable given that the experiment is performed in a collision energy window where the ratio of the elastic

<sup>\*</sup>sourav@rri.res.in<sup>†</sup>Present address: Department of Physics, Indian Institute of Science Education and Research (IISER) Bhopal, Bhopal – 462066, India.

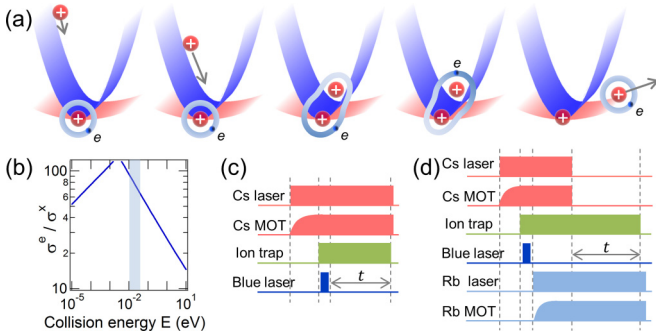


FIG. 1. (a) Pictorial representation of ion cooling by RCE. The Paul trap for ions is much deeper than the cocentered MOT for atoms. As the ion approaches the center of the Paul trap, its secular speed increases and it collides with an atom at rest. During the collision, the outermost electron wave function is shared among both species, thus allowing RCE. Postcollision, the fast moving atom is ejected from the MOT and a very cold ion occupies the center of the Paul trap. (b) The theoretically calculated [17,29,30] ratio of elastic to RCE cross section for the Cs-Cs<sup>+</sup> system. The behavior of  $\sigma^x$  changes from logarithmic in  $E$  at high  $E$  to  $E^{-1/2}$  below a few meV [34], resulting in a sharp change in the trend of  $\sigma^e/\sigma^x$ . The shaded area represents the collision energy regime of the present experiments. (c) Timing sequence for the Cs-Cs<sup>+</sup> experiments. Results are presented in Fig. 2. (d) Timing sequence for the Rb-Cs<sup>+</sup> experiments. Results are presented in Figs. 3 and 4.

cross section ( $\sigma^e$ ) to the RCE cross section ( $\sigma^x$ ) is close to its maximum [see Fig. 1(b)], favoring elastic collisions by a factor of  $\sim 70$  [17,29,30]. The cooling of ions by RCE is not restricted to ions trapped in a Paul trap, where micromotion sets a limit to the lowest ion temperature that can be reached in a hybrid trap [6,31], and could possibly be extended to ions trapped in an optical dipole trap [32] where no such limitations exist.

*Experimental setup.* The apparatus [9,11,33] consists of a Paul trap for Cs<sup>+</sup> ions and MOTs for ultracold Cs and Rb atoms. Details of the MOTs and the Paul trap are provided in the Supplemental Material [34]. The Paul trap is well centered with the MOTs to ensure the most efficient cooling [9–11]. The  $1/e^2$  radius ( $= 470 \pm 25 \mu\text{m}$ ) of the Cs and Rb MOTs is similar for all experiments. The MOT atom number ( $\sim 5\text{--}10 \times 10^6$ ), and consequently the peak density ( $n$ ), is tuned by changing the current through the atomic dispenser sources. To load the ion trap, a blue 473-nm laser is used to ionize Cs atoms in the  $6P_{3/2}$  state that are already present in a Cs MOT. The ions are detected using a channel electron multiplier (CEM) and the time of flight (TOF) to the detector is used to differentiate ions of different species.

*Cooling of Cs<sup>+</sup> ions by ultracold Cs atoms.* The experimental sequence is depicted in Fig. 1(c). First, the shutter in the path of the Cs laser beams is opened and a Cs MOT is allowed to load until saturation, and then the rf and dc ion trap voltages are turned on, and Cs<sup>+</sup> ions are created by briefly turning on the blue laser which loads  $\sim 1000$  Cs<sup>+</sup> ions in the ion trap. Subsequently, either the shutter is kept open, allowing the Cs<sup>+</sup> ions to interact with the Cs MOT atoms, or the shutter is closed, emptying the Cs MOT. The ions are held in the ion trap for a predetermined hold time  $t$  and then the surviving ions are extracted from the ion trap and detected using the CEM.

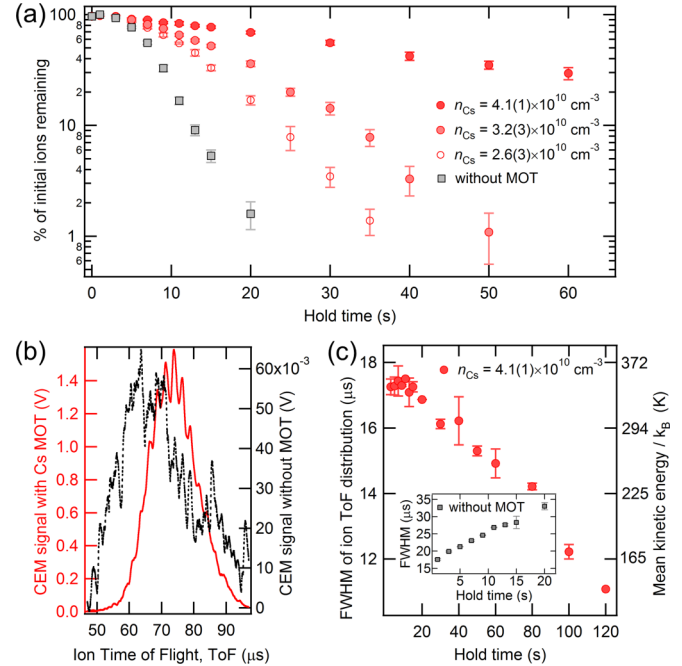


FIG. 2. (a) Decay of Cs<sup>+</sup> ions from the ion trap when held with (circles) and without (squares) a Cs MOT. The lifetime of Cs<sup>+</sup> ions in the ion trap increases as the Cs MOT density  $n_{Cs}$  increases. The increase in lifetime is due to cooling of trapped Cs<sup>+</sup> ions by Cs atoms in the MOT. (b) The CEM signal when ions are extracted after 15 s of hold time either in the presence of a Cs MOT (solid line, left axis) or in the absence of a MOT (dotted line, right axis). The width of the ion TOF distribution is lower in presence of a Cs MOT. The peak position shifts to higher TOF for colder ions due to paraxial lensing. (c) In the presence of a Cs MOT, the FWHM of the ion TOF distribution (obtained by fitting to a Gaussian function) decreases as the hold time increases, suggesting cooling of ions by the Cs atoms. The ions' mean kinetic energy (in temperature units) is plotted on the right axis. Inset: In the absence of a Cs MOT, the FWHM of the ion TOF distribution increases as the hold time increases, signifying the heating of ions.

The hold time is changed and the sequence is repeated. The experiment is then repeated for different values of Cs MOT density ( $n_{Cs}$ ).

The result of the experiments is shown in Fig. 2. Note that, for Figs. 2–4, standard deviation ( $1\sigma$ ) error bars are shown and are smaller than the data points where not visible. From Fig. 2(a), it is clear that the lifetime of the Cs<sup>+</sup> ions in the ion trap increases when a Cs MOT is present. This is due to the cooling (i.e., reduction in secular speed) of Cs<sup>+</sup> ions by collisions with Cs MOT atoms. Here, secular speed refers to the speed of an ion oscillating at its secular frequency. The cooling of ions occurs because the atoms are localized in a region much smaller than the volume occupied by the ions and are placed precisely at the center of the ion trap—a geometry that always results in a reduction of the secular speed of a trapped ion after collision, thereby cooling the ion [9,11]. Figure 2(a) also shows that the cooling effect increases as the Cs MOT density  $n_{Cs}$  increases. This is a result of an increase in the ion-atom collision rate as  $n_{Cs}$  increases, leading to more efficient ion cooling.

In Fig. 2(b) we show an example of the ion TOF distribution, at hold time  $t = 15$  s, for the “with MOT” and “without MOT” cases—the full width at half maximum (FWHM) of the distribution reduces when the Cs MOT is present, providing independent evidence of ion cooling. The FWHM reduces because the extent of the secular orbit of a trapped ion is reduced due to ion cooling by the MOT atoms, resulting in compression in the phase space. Figure 2(c) shows that the FWHM of the ions’ TOF distribution keeps reducing as the hold time increases—a result of a systematic reduction in the ions’ mean kinetic energy due to cooling by the MOT atoms. See the Supplemental Material [34] for details regarding the determination of the ion temperature. Note that in the absence of the MOT, the FWHM increases with increasing hold time [inset of Fig. 2(c)], suggesting the heating of ions due, primarily, to trap imperfections and, to a much lower extent, to collisions with the background gas.

*Rationale for the Rb-Cs<sup>+</sup> experiment.* While the above results confirm Cs<sup>+</sup> ion cooling by Cs MOT atoms, there is no experimental signature that can distinguish between the EC and the RCE channels for cooling. For the discriminatory test, we cool trapped Cs<sup>+</sup> ions with ultracold Rb atoms. Since Cs<sup>+</sup> and Rb are different species, RCE between Cs<sup>+</sup> and Rb is not possible. Moreover, related calculations [35], related experiments [11], and the results below show that the rate of nonresonant charge exchange (nRCE) at a low ( $\ll 1$  eV) collision energy is negligible. Therefore, for the cooling of Cs<sup>+</sup> ions by Rb MOT, the ion cooling is through ECs only, which is explained accurately by theoretical models [25,26]. The EC cooling rates ( $k_{\text{Cs}}^e, k_{\text{Rb}}^e$ ) in these models depend on the atom-ion mass ratios ( $\xi = 1.00, \xi = 0.64$ ) and the EC cross sections ( $\sigma_{\text{Cs}}^e, \sigma_{\text{Rb}}^e$ ) [29] for the two cases (Cs-Cs<sup>+</sup>, Rb-Cs<sup>+</sup>). The effective ratio of the EC cross section is  $(\sigma_{\text{Cs}}^e/\sigma_{\text{Rb}}^e)_{\text{eff}} = 1.23$  (see Supplemental Material [34]). For our MOTs, which are localized but finite in size, the model [25,26] predicts  $0.62 \lesssim (k_{\text{Cs}}^e/k_{\text{Rb}}^e) \lesssim 1.28$  (see Ref. [34]). Thus, the theoretical (th) upper bound (ub) is  $(k_{\text{Cs}}/k_{\text{Rb}})_{\text{th}}^{\text{ub}} = 1.28$ —an experimental value higher than this would bring out the role of RCE. Here,  $k_{\text{Cs}}$  and  $k_{\text{Rb}}$  are the total (EC+RCE) cooling rates for the Cs-Cs<sup>+</sup> and Rb-Cs<sup>+</sup> cases, respectively.

*Cooling of Cs<sup>+</sup> ions by ultracold Rb atoms.* The experimental sequence is depicted in Fig. 1(d) and is similar to the Cs-Cs<sup>+</sup> experiments, but with one preparation difference. After the loading of the Cs<sup>+</sup> ions, the Cs MOT is kept operative and the Rb laser beams are allowed in, and the Rb MOT is allowed to load until saturation. During this time, which is 10 s, the Cs<sup>+</sup> ions interact with both the Cs and the Rb MOTs. Instead, if the Cs MOT is emptied immediately after the Cs<sup>+</sup> ions are loaded, there is a severe loss of Cs<sup>+</sup> ions [see the “without MOT” case in Fig. 2(a)], while the Rb MOT loads. After a 10-s duration (this is taken to be  $t = 0$  s), the Cs MOT (Rb MOT) is emptied by blocking the Cs (Rb) laser beams and the Cs<sup>+</sup> ions are held in the presence of the Rb MOT (Cs MOT) for a variable hold time  $t$  to get the ion decay curve with Rb MOT (with Cs MOT). Both MOTs are emptied at  $t = 0$  s to get the “without MOT” data. The surviving ions are detected using the CEM and the number of ions and the FWHM of the ion TOF distribution determined. Notably, the detected ion TOF distribution is consistent with Cs<sup>+</sup> ions and not consistent with the TOF profile of Rb<sup>+</sup> ions (on average, Rb<sup>+</sup> ions would arrive

14  $\mu\text{s}$  before the Cs<sup>+</sup> ions). No confirmed detection of Rb<sup>+</sup> ions could be made even when the ion trap parameters were adjusted to trap Rb<sup>+</sup> ions efficiently—we therefore conclude that all detected ions are Cs<sup>+</sup> and that nRCE (Cs<sup>+</sup> + Rb  $\rightarrow$  Cs<sup>+</sup>Rb<sup>+</sup>) rates are very small.

In Fig. 3 we plot the number of Cs<sup>+</sup> ions detected at different hold times when the ions are held in the presence and absence of the Rb or Cs MOT. The density of Rb MOT [ $n_{\text{Rb}} = 4.0(1) \times 10^{10} \text{ cm}^{-3}$ ] is similar to the density of the Cs MOT [ $n_{\text{Cs}} = 3.8(2) \times 10^{10} \text{ cm}^{-3}$ ]. Compared to the “without MOT” case, a larger number of Cs<sup>+</sup> ions survive when the Rb MOT is present—this is due to cooling by ECs with ultracold Rb atoms. The experiment with Cs<sup>+</sup> ions in the presence of a Cs MOT results in an even longer ion lifetime. On fitting the  $t \geq 8$  s data to an expression of the form  $Ae^{-\gamma t}$ , we get  $\gamma_0 = 0.34(1) \text{ s}^{-1}$ ,  $\gamma_{\text{Rb}} = 0.17(1) \text{ s}^{-1}$ , and  $\gamma_{\text{Cs}} = 0.047(3) \text{ s}^{-1}$  for the “without MOT,” the “with Rb MOT,” and the “with Cs MOT” cases, respectively.  $\gamma_0$ ,  $\gamma_{\text{Rb}}$ , and  $\gamma_{\text{Cs}}$  depend on the ion heating rates in the respective cases, therefore,  $-(\gamma_{\text{Cs}} - \gamma_0)$  and  $-(\gamma_{\text{Rb}} - \gamma_0)$  represent the cooling due to the Cs MOT and Rb MOT, respectively. The ratio  $(\gamma_{\text{Cs}} - \gamma_0)/(\gamma_{\text{Rb}} - \gamma_0) = 1.72(2)$  provides an experimental estimate of  $(k_{\text{Cs}}/k_{\text{Rb}})$ , and is higher than the theoretical upper bound  $(k_{\text{Cs}}/k_{\text{Rb}})_{\text{th}}^{\text{ub}} = 1.28$  based on ECs only. We therefore conclude that an additional cooling channel is active in the Cs-Cs<sup>+</sup> case and it must be RCE since it can bring a fast Cs<sup>+</sup> ion to rest in a single ion-atom collision [see Fig. 1(a)].

This cooling beyond the bounds of EC cooling must be attributed to a different process. There are only two mechanisms, other than RCE, which need to be considered. The first mechanism is one in which a fast ion collides with an atom at rest and kinetically excites the atom to an excited electronic state. Such a collision could result in ion cooling. However, such collisions are energetically forbidden in our experiment since the mean kinetic energy of a trapped ion is  $< 0.05$  eV, whereas the minimum energy required for an electronic excitation ( $6S_{1/2} \rightarrow 6P_{1/2}$ ) of Cs is  $\sim 1.39$  eV. The other mechanism is one in which a fast ion collides with an atom at rest and transfers its kinetic energy, resulting in a hyperfine excitation in the atom. A single atomic hyperfine changing

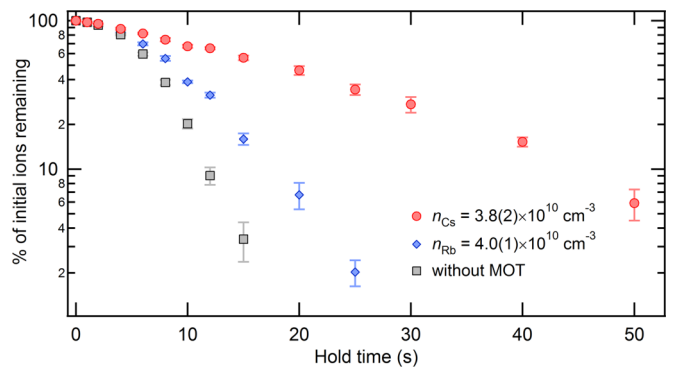


FIG. 3. Decay of Cs<sup>+</sup> ions from the ion trap when held with a Rb MOT (rhombuses), a Cs MOT (circles), or without any MOT (squares). The lifetime Cs<sup>+</sup> in the ion trap increases in the presence of either of the two MOTs, but the enhancement in lifetime is higher when the Cs MOT is present. The densities of the Cs and Rb MOTs are similar.

collision can change the energy of the ion by only  $\sim 38 \mu\text{eV}$  ( $\equiv 9.2 \text{ GHz}$  atomic hyperfine splitting). However, if active, in our experiments the atomic hyperfine state changing collisions would be a heating mechanism for the ions. This is because the atoms in a MOT are in the upper ( $6S_{1/2} F = 4$ ) hyperfine state and therefore would transfer energy to the ion while making a transition to the lower ( $6S_{1/2} F = 3$ ) hyperfine state. The electronic or hyperfine state changing collisions therefore cannot explain the observed cooling. Further, the results of the experiment are in good agreement with the expectations of cooling due to the RCE process, allowing us to attribute the faster cooling in the Cs-Cs<sup>+</sup> case to the RCE process.

*Quantifying the RCE cooling rate.* The above determination of  $(k_{\text{Cs}}/k_{\text{Rb}})$  based on a difference in the ion lifetime depends on the fitted equation. To avoid this model dependence, we develop an alternative experimental strategy to quantify the role of RCE. We tune  $n_{\text{Cs}}$  and  $n_{\text{Rb}}$  to determine a pair of values for which the ion decay curves for both the Cs-Cs<sup>+</sup> and Rb-Cs<sup>+</sup> cases are essentially identical [Fig. 4(a)]. This is observed to occur when the ratio  $n_{\text{Rb}}/n_{\text{Cs}} = 2.0(2)$ . Further, it is seen that at each hold time the FWHM of the TOF distributions for the two cases also coincide [Fig. 4(b)], suggesting matched cooling rates under these conditions. Since  $k_{\text{Rb}} \propto n_{\text{Rb}}$  and  $k_{\text{Cs}} \propto n_{\text{Cs}}$ , these figures suggest that  $(k_{\text{Cs}}/k_{\text{Rb}}) = 2.0(2)$ . This value is close to  $1.72(2)$  obtained earlier and is higher than  $1.28$ , confirming that cooling by RCE is active in the Cs-Cs<sup>+</sup> case. Thus  $k_{\text{Cs}}$  has contributions from both ECs ( $k_{\text{Cs}}^{\text{e}}$ ) and RCE ( $k_{\text{Cs}}^{\text{x}}$ ), i.e.,  $k_{\text{Cs}} = k_{\text{Cs}}^{\text{e}} + k_{\text{Cs}}^{\text{x}}$ , while  $k_{\text{Rb}}$  has a contribution only from ECs, i.e.,  $k_{\text{Rb}} = k_{\text{Rb}}^{\text{e}}$ . So, we have  $(k_{\text{Cs}}^{\text{e}} + k_{\text{Cs}}^{\text{x}}) = 2 k_{\text{Rb}}^{\text{e}}$ . On using  $0.62 \lesssim (k_{\text{Cs}}^{\text{e}}/k_{\text{Rb}}^{\text{e}}) \lesssim 1.28$  (see Ref. [34]), we get  $0.56 \lesssim (k_{\text{Cs}}^{\text{x}}/k_{\text{Cs}}^{\text{e}}) \lesssim 2.23$ , i.e., the effective cooling rates for cooling by RCE and cooling by ECs are of similar magnitude. However, as discussed below, the cooling efficiency for a single collision is much greater in the case of RCE cooling.

The cooling rate  $k_{\text{Cs}}$  can be defined as  $k_{\text{Cs}} \equiv k_{\text{Cs}}^{\text{e}} + k_{\text{Cs}}^{\text{x}} \approx \delta E_{\text{Cs}}^{\text{e}} n_{\text{Cs}} \sigma_{\text{Cs}}^{\text{e}} v + \delta E_{\text{Cs}}^{\text{x}} n_{\text{Cs}} \sigma_{\text{Cs}}^{\text{x}} v$ , where  $\delta E_{\text{Cs}}^{\text{x}}$  ( $\delta E_{\text{Cs}}^{\text{e}}$ ) is the

energy lost by a Cs<sup>+</sup> ion in a single RCE (EC) collision with a Cs atom (see Ref. [34]),  $\sigma_{\text{Cs}}^{\text{x}}$  ( $\sigma_{\text{Cs}}^{\text{e}}$ ) is the RCE (EC) cross section, and  $v$  is the speed of the ion before collision. Taking a ratio between  $k_{\text{Cs}}^{\text{x}}$  and  $k_{\text{Cs}}^{\text{e}}$ , we get  $\delta E_{\text{Cs}}^{\text{x}}/\delta E_{\text{Cs}}^{\text{e}} = (\sigma_{\text{Cs}}^{\text{e}}/\sigma_{\text{Cs}}^{\text{x}})(k_{\text{Cs}}^{\text{x}}/k_{\text{Cs}}^{\text{e}})$ . The theoretically calculated value of  $(\sigma_{\text{Cs}}^{\text{e}}/\sigma_{\text{Cs}}^{\text{x}})$  varies non-monotonically with collision energy [17,29,30] with maxima ( $\sim 100$ ) around the 10-meV collision energy [see Fig. 1(b)]. Our experiments are conducted near this region at collision energies of  $\sim 30 \text{ meV}$  ( $\equiv 350 \text{ K}$ ), where  $(\sigma_{\text{Cs}}^{\text{e}}/\sigma_{\text{Cs}}^{\text{x}}) \sim 69$  [17,29,30]. On using  $0.56 \lesssim (k_{\text{Cs}}^{\text{x}}/k_{\text{Cs}}^{\text{e}}) \lesssim 2.23$  obtained above, we get  $39 \lesssim \delta E_{\text{Cs}}^{\text{x}}/\delta E_{\text{Cs}}^{\text{e}} \lesssim 154$ . The result shows that the cooling per RCE collision is dramatically more efficient than cooling per EC. This is consistent with the hopping of an electron from the parent atom to the daughter ion in a single collision and results in rapid cooling despite the lower RCE cross section.

*Comments from supplementary experiments.* We conducted control experiments with Cs-Rb<sup>+</sup> and Rb-Rb<sup>+</sup> and found that cooling in the Rb-Rb<sup>+</sup> case is more efficient. While this is suggestive of cooling by RCE in the Rb-Rb<sup>+</sup> case, the data presented in Figs. 3 and 4 are a better demonstration of RCE. This is because even when considering only ECs, one expects that the cooling of Rb<sup>+</sup> by Rb will be more efficient than the cooling of Rb<sup>+</sup> by Cs, since cooling by ECs is more effective when the mass of the neutral atom is lower [25,26]. We have also conducted experiments with Rb-Cs<sup>+</sup> and Rb-Rb<sup>+</sup> and found cooling to be more efficient in the latter, suggesting the presence of the additional RCE cooling mechanism in the homonuclear Rb-Rb<sup>+</sup> case.

*Conclusion.* In conclusion, we demonstrate a very efficient method of ion cooling based on RCE. We show the cooling of Cs<sup>+</sup> ions, trapped in a Paul trap, by collisions with localized, precisely centered, ultracold Cs and Rb atoms trapped in their respective MOTs. The cooling of Cs<sup>+</sup> ions by Cs atoms is more efficient than the cooling by Rb atoms, the reason for which is RCE in the former case—similar cooling should occur in all other parent-daughter systems. The experimentally determined per-collision cooling in case of RCE is found to be two orders of magnitude higher than cooling by EC. This has direct implications for reaching the ultracold temperature regime, i.e.,  $100 \mu\text{K}$  or lower, in ion-atom collisions. For example, in the absence of ion heating mechanisms, an ion at  $350 \text{ K}$  would require  $\sim 240$  ECs to cool down to  $100 \mu\text{K}$ , whereas the same effect can result from a single RCE collision. Our findings also suggest that an ion can be cotrapped with atoms for very long durations if a sufficiently dense and localized gas of ultracold atoms is available, thereby allowing controlled studies of ion-atom collisions. The result also establishes the experimental basis for future experiments on charge mobility [16], mesoscopic molecular ions [19], and impurity physics in many-body systems.

*Acknowledgments.* We are happy to acknowledge helpful discussions with Daniel Comparat, Olivier Dulieu, and Anders Kastberg. S.A.R. acknowledges support from the Indo-French Centre for the promotion of Advanced Research-CEFIPRA, Project No. 5404-1. S.D. acknowledges support from the Department of Science and Technology (DST), India in the form of the DST-INSPIRE Faculty Award (IFA14-PH-114).

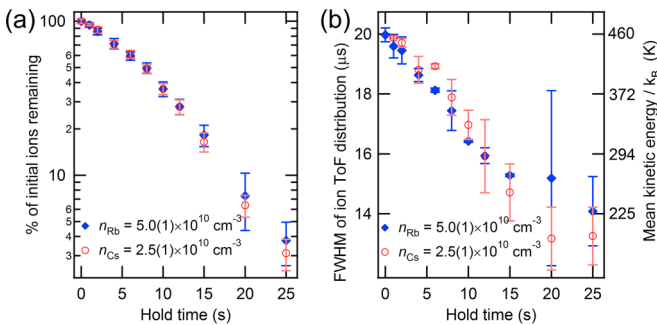


FIG. 4. (a) Decay of Cs<sup>+</sup> ions from the ion trap when held in the presence of a Rb MOT (rhombuses) of density  $n_{\text{Rb}} = 5.0(1) \times 10^{10} \text{ cm}^{-3}$  or in the presence of a Cs MOT (circles) of density  $n_{\text{Cs}} = 2.5(1) \times 10^{10} \text{ cm}^{-3}$ . The decay curves are essentially identical. (b) The FWHM of the ion TOF distribution, and the corresponding mean kinetic energy plotted on the right axis, when held in the presence of a Rb MOT (rhombuses) or in the presence of a Cs MOT (circles). The FWHM of the ion TOF distribution decreases as the hold time increases, suggesting the cooling of ions in both cases and at similar rates.

- [1] A. D. Ludlow, M. M. Boyd, J. Ye, E. Peik, and P. O. Schmidt, *Rev. Mod. Phys.* **87**, 637 (2015).
- [2] W. M. Itano, J. C. Bergquist, J. J. Bollinger, and D. J. Wineland, *Phys. Scr.* **T59**, 106 (1995).
- [3] A. T. Grier, M. Cetina, F. Oručević, and V. Vuletić, *Phys. Rev. Lett.* **102**, 223201 (2009).
- [4] C. Zipkes, S. Palzer, C. Sias, and M. Köhl, *Nature (London)* **464**, 388 (2010).
- [5] S. Schmid, A. Härter, and J. Hecker Denschlag, *Phys. Rev. Lett.* **105**, 133202 (2010).
- [6] Z. Meir, T. Sikorsky, R. Ben-shlomi, N. Akerman, Y. Dallal, and R. Ozeri, *Phys. Rev. Lett.* **117**, 243401 (2016).
- [7] L. Ratschbacher, C. Zipkes, C. Sias, and M. Köhl, *Nat. Phys.* **8**, 649 (2012).
- [8] S. Haze, R. Saito, M. Fujinaga, and T. Mukaiyama, *Phys. Rev. A* **91**, 032709 (2015).
- [9] K. Ravi, S. Lee, A. Sharma, G. Werth, and S. A. Rangwala, *Nat. Commun.* **3**, 1126 (2012).
- [10] I. Sivarajah, D. S. Goodman, J. E. Wells, F. A. Narducci, and W. W. Smith, *Phys. Rev. A* **86**, 063419 (2012).
- [11] S. Dutta, R. Sawant, and S. A. Rangwala, *Phys. Rev. Lett.* **118**, 113401 (2017).
- [12] F. H. J. Hall, M. Aymar, N. Bouloufa-Maafa, O. Dulieu, and S. Willitsch, *Phys. Rev. Lett.* **107**, 243202 (2011).
- [13] A. Krükov, A. Mohammadi, A. Härter, J. Hecker Denschlag, J. Pérez-Ríos, and C. H. Greene, *Phys. Rev. Lett.* **116**, 193201 (2016).
- [14] S. Dutta and S. A. Rangwala, *Phys. Rev. A* **94**, 053841 (2016).
- [15] W. G. Rellergert, S. T. Sullivan, S. J. Schowalter, S. Kotochigova, K. Chen, and E. R. Hudson, *Nature (London)* **495**, 490 (2013).
- [16] R. Côté, *Phys. Rev. Lett.* **85**, 5316 (2000).
- [17] R. Côté and A. Dalgarno, *Phys. Rev. A* **62**, 012709 (2000).
- [18] G. Heiche and E. A. Mason, *J. Chem. Phys.* **53**, 4687 (1970).
- [19] R. Côté, V. Kharchenko, and M. D. Lukin, *Phys. Rev. Lett.* **89**, 093001 (2002).
- [20] A. Rakshit and B. Deb, *Phys. Rev. A* **83**, 022703 (2011).
- [21] Z. Idziaszek, T. Calarco, P. S. Julienne, and A. Simoni, *Phys. Rev. A* **79**, 010702(R) (2009).
- [22] R. G. De Voe, *Phys. Rev. Lett.* **102**, 063001 (2009).
- [23] C. Zipkes, L. Ratschbacher, C. Sias, and M. Köhl, *New J. Phys.* **13**, 053020 (2011).
- [24] K. Chen, S. T. Sullivan, and E. R. Hudson, *Phys. Rev. Lett.* **112**, 143009 (2014).
- [25] B. Höltkemeier, P. Weckesser, H. López-Carrera, and M. Weidemüller, *Phys. Rev. Lett.* **116**, 233003 (2016).
- [26] B. Höltkemeier, P. Weckesser, H. López-Carrera, and M. Weidemüller, *Phys. Rev. A* **94**, 062703 (2016).
- [27] J. Perel, R. H. Vernon, and H. L. Daley, *Phys. Rev.* **138**, A937 (1965).
- [28] X. Flechard, H. Nguyen, E. Wells, I. Ben-Itzhak, and B. D. DePaola, *Phys. Rev. Lett.* **87**, 123203 (2001).
- [29] J. Mitroy, M. S. Safronova, and C. W. Clark, *J. Phys. B: At., Mol. Opt. Phys.* **43**, 202001 (2010).
- [30] B. M. Smirnov, *Phys.-Usp.* **44**, 221 (2001).
- [31] M. Cetina, A. T. Grier, and V. Vuletić, *Phys. Rev. Lett.* **109**, 253201 (2012).
- [32] A. Lambrecht, J. Schmidt, P. Weckesser, M. Debatin, L. Karpa, and T. Schaetz, *Nat. Photonics* **11**, 704 (2017).
- [33] K. Ravi, S. Lee, A. Sharma, G. Werth, and S. A. Rangwala, *Appl. Phys. B* **107**, 971 (2012).
- [34] See Supplemental Material at <http://link.aps.org/supplemental/10.1103/PhysRevA.97.041401> for details regarding the experimental setup, estimation of ion temperature, theoretical values of ion-atom collision cross sections, and theoretical estimate for the EC cooling rate.
- [35] L. L. Yan, L. Liu, Y. Wu, Y. Z. Qu, J. G. Wang, and R. J. Buenker, *Phys. Rev. A* **88**, 012709 (2013).